

Role of Depletion and Surface-Induced Structural Forces in Bidisperse Suspensions

W. Xu, A. D. Nikolov, and D. T. Wasan

Dept. of Chemical Engineering, Illinois Institute of Technology, Chicago, IL 60616

Depletion and structural interactions between dilute, large, nearly hard-sphere colloidal particles in a fluid dispersion containing much smaller nearly hard spheres were investigated as a function of small-particle concentration in sedimentation experiments. It shows that low concentrations of fine particles can destabilize larger particles due to the attractive depletion forces, while at higher concentrations of small particles, the surface-induced structural forces prevent large-size particles from approaching each other and thereby stabilize the large-particle suspension. A theoretical model based on the Ornstein–Zernike method was used to calculate the interparticle interactions in a bidispersed colloidal system in which small particles are polydispersed. The theoretical results explain the experimental observations.

Introduction

Most of the theories that have been presented on forces acting between suspended colloidal particles are concerned with the van der Waals force and a force caused by electrical layers surrounding the particles. These theories can explain many phenomena observed in experiments relating to the stability of suspended particles and are now widely accepted. Forces of other origins, however, can also act between the particles. In recent years, depletion interactions that result from the collective behavior of a many-body system have received increased attention from many researchers (Gast et al., 1983; Tadros, 1990; Richetti and Kekicheff, 1992; Liang et al., 1993; Seebergh and Berg, 1994; Walz and Sharma, 1994; Mao et al., 1995; Dickinson et al., 1995). Depletion forces arise between spheres suspended in a solution of nonadsorbing polymers, micelles, or hard spheres. The last case is amenable to detailed analysis, and serves as a model for the others. The depletion forces arise whenever the concentration of nonadsorbing polymers, micelles, or hard spheres in the gap region between two particles becomes different from the bulk. For example, at small gap widths, the nonadsorbing polymers, micelles, or hard spheres are excluded from the gap, resulting in an attractive force due to the difference in osmotic pressure.

Numerous theoretical and experimental investigations on depletion interactions have been reported. The first satisfactory explanation of the depletion effect was given by Asakura

and Oosawa (1954), who considered the case of two parallel plates and two spherical particles or macromolecules in a solution of rigid spherical molecules. When the distance between two parallel plates is less than the diameter of the surrounding macromolecules, the macromolecules are excluded from the region between the plates. The osmotic pressure in this region then becomes lower than that outside the plates, and a net attraction develops. Although relatively simple, this hard-sphere/hard-wall interaction has been successfully used to predict the onset of phase separation in a wide variety of colloidal systems. In a later article, Asakura and Oosawa (1958) calculated the depletion interaction between two spherical and charged spherical macromolecules. For the latter case, an approximate model was developed predicting both the depletion force and energy as a function of macromolecule concentration and solution ionic strength.

In the experimental study of stability of colloidal suspensions in the presence of free polymers, Feigin and Napper (1980) noticed that the free polymer not only can destabilize the colloidal suspensions by producing an attractive depletion interaction, but can also stabilize the system under certain conditions. From these observations, they proposed an approximate theory of stabilization and depletion flocculation of colloidal particles by polymers in free solution. It was reported that a reasonable agreement between theory and experiment was achieved for the critical volume fractions of polymer required to induce both depletion flocculation and stabilization.

Correspondence concerning this article should be addressed to D. T. Wasan.

The depletion effect induced by micelles was investigated by numerous researchers (Aronson, 1989, 1991, 1992; Bibette et al., 1990; Bibette, 1991; Dickinson et al., 1997). In their research, they found that at high surfactant micellar concentrations, a "creaming" of the emulsion was observed and the emulsion was destabilized. They demonstrated that this behavior was related to a fluid-solid phase transition due to an attractive interaction induced by the depletion of surfactant micelles.

Sanyal and coworkers (1992) presented a simple experimental method to prove the existence of the depletion force. In their experiment, a binary aqueous suspension of large and small nearly hard-sphere colloidal polystyrene spheres (size ratio 5:1) was allowed to settle in a container for 2–3 days at room temperature. They directly observed the flocculated larger particles in the sediment with an optical microscope. It was found that at certain volume fraction ratios (large particles/small particles), the large particles flocculated due to the depletion mechanism.

A systematic theoretical study of depletion and structural forces in colloidal dispersions was conducted by Chu and colleagues (1994, 1995, 1996). In their research, they calculated the effective interactions from the radial distribution function by solving the Ornstein–Zernike (O–Z) equation. For a simple binary mixture of large and small particles, the calculated effective interaction between two large (colloidal) particles is found to be oscillatory in general, including both the Asakura–Oosawa-type attractive depletion well and the repulsive energy barrier (which is caused by the formation of small-particle layers between the two large particles). Both depletion (i.e., volume exclusion effect) and surface-induced, long-range structural forces due to small particles are included in this effective interaction that is concentration-dependent. A parametric study was also conducted to examine the relation between the effective interaction potential and controllable parameters such as particle concentration and size ratio. The effect of polydispersity of small particles on both depletion and structural forces was also addressed in their study, and they found that polydispersity affects the structural energy barrier more than it does the attractive depletion well. The structural force arising from the presence of small-particle layering phenomenon and the in-layer structure formation can stabilize the dispersion in a certain time scale, depending on the magnitude of the structural energy barrier.

As a special case of a bidispersed system, when the size ratio of large to small particles approaches infinity, the structuring phenomenon of small colloidal particles or micelles inside thin liquid films has been studied extensively both experimentally (Nikolov and Wasan, 1989, 1992, 1996, 1997; Bashcheva et al., 1992; Koczo et al., 1996) and theoretically (Nikolov et al., 1989; Bergeron and Radke, 1992; Chu et al., 1994, 1995). It was found that at high concentrations of micelles or submicron colloidal particles (due to the layering and in-layer ordering structure formation inside free liquid films), the structural disjoining pressure exerted by micelles or particles in a thin liquid film becomes oscillatory, and it can be positive or negative depending on the thickness of the film. Thus, liquid films thin in a stepwise fashion that affects film stability.

Depletion destabilization and structural stabilization phe-

nomena have been directly observed in sedimentation experiments for a bidispersed system (Chu et al., 1996). However, in their experiment, the latex particles were charged and the charge density was unknown, therefore, the experimental results could not be compared directly with the theoretical prediction.

The main purpose of this article is to experimentally and theoretically study the depletion and structural forces between nearly hard spheres for a bidisperse particle suspension. Sedimentation experiments of silica dispersions were conducted, and the normalized sedimentation speed U/U_0 was obtained. By correcting the experimental data (taking into account the effect of hydrodynamic interactions between particles), we were able to observe the effects of depletion and structural forces on the stability of colloidal dispersions. Finally, these experimental results were compared with theoretical predictions.

Experimental Studies

Sedimentation measurements

For the setting-rate studies, a cylindrical flat-bottomed glass tube, 85 mm long by 23 mm diameter, was used. Sedimentation measurements are extremely sensitive to temperature changes and vibration. They cause convections that complicate the analysis of sedimentation velocities. To prevent convections, the sedimentation tubes were isolated and mounted on a vibration-free table. The equipment was placed in a temperature-controlled room at a constant $20 \pm 0.1^\circ\text{C}$. As soon as the meniscus of the settling particles had separated from the air–water interface, the movement of the separation boundary was measured as a function of time. The movement was followed over a drop of at least 2 cm. The time of settling varied between 20 and 200 h, depending on the concentration and density of particles.

Capillary force balance

In order to estimate the effective volume fractions of small silica particles, the capillary force balance technique described in our recent article (Nikolov and Wasan, 1996) was employed. Microscopic films were formed in a cylindrical capillary with a hydrophilic inner wall with a radius of $R_c = 1.5$ mm. The films were formed by sucking out the liquid from a biconcave drop inside the capillary through an orifice in the wall. The resulting horizontal flat film is encircled by a biconcave meniscus. The radius of the film ($r_c = 0.3$ mm) is kept constant by controlling the capillary pressure P_c in the meniscus. In fact, the changes in P_c during the thinning of the film were negligible: in these experiments, $R_c \gg r_c$, and the contact angle subtended between the film and meniscus is less than 1° .

The entire assembly is placed on the stage of a differential interference microscope (Epival Interphako), which is mounted on a vibration-free table to keep any external disturbances from affecting the film-thinning process. Monochromatic light (wavelength 546 nm) from the top of the glass cell is incident on the film surface, and the light reflected from a small portion of the thinning-film area is conducted through a fiber-optic probe to a photomultiplier. Here the optical signal is converted to an electrical signal,

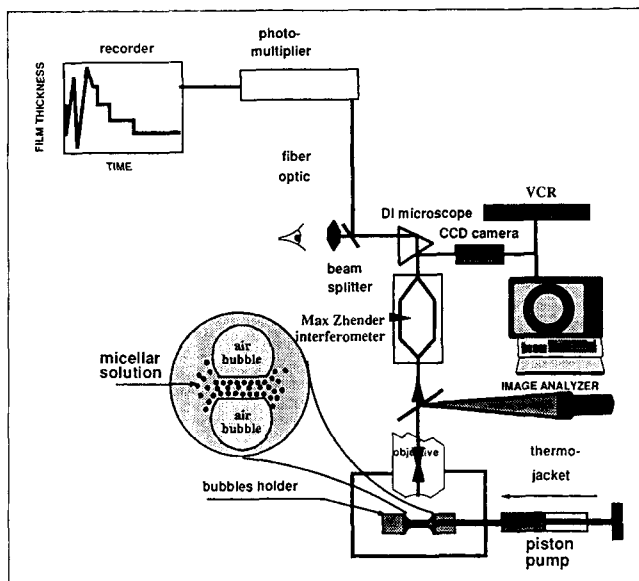


Figure 1. Capillary-force balance technique.

amplified through an electrometer, and finally recorded on a strip-chart recorder that represents photocurrent as a function of time. The video in conjunction with a monitor and VCR records, in detail, the process of film thinning. The experimental setup is shown in Figure 1.

Materials

Silica dispersions were selected as our experimental systems. The low surface-charge silica (surface-charge density lower than 0.004 milliequivalent (meq OH/g SiO₂) dispersions were produced by Nissan Chemical Industries, Ltd. Two different-sized silica particles were used: a large particle of diameter 330 nm with polydispersity (standard deviation) less than 5%, and a small-silica particle of effective diameter 38 nm with the polydispersity near 15%. The effective volume fractions of small-silica dispersions, which were used in our theoretical calculations, were determined by the capillary-force-balance technique based on the principle of the stepwise jump transitions during the film-thinning process (Nikolov and Wasan, 1992; Chu et al., 1994). It was found that the microscopic horizontal film (film diameter 0.6 mm) formed from 29% (physical) volume fraction of small-silica dispersion showed four stepwise transitions during the film-thinning process. The effective hard sphere volume fraction corresponding to these four stepwise transitions was then estimated to be around 38 vol % according to computer simulation (Chu et al., 1994). This difference of volume fraction results from the small but finite charge on the silica, creating a double layer around the particles.

Deionized distilled water was used to make dispersions in all of the experiments.

Theoretical Studies

Sedimentation

The sedimentation velocity, U_0 , of a particle of an arbitrary shape at infinite dilution is given by Stokes' law in the form

$$U_0 = \frac{V_p(\rho_p - \rho_0)g}{f}, \quad (1)$$

where V_p is the particle volume; ρ_p the particle density; ρ_0 the solvent density; g the gravitational acceleration; and f the friction coefficient of the particle. The sedimentation velocity of a spherical particle of radius R , for which $V_p = (4/3)\pi R^3$ and Stokes' friction $f = 6\pi\eta_0 R$, in a solvent with viscosity η_0 , is

$$U_0 = \frac{2R^2(\rho_p - \rho_0)g}{9\eta_0}. \quad (2)$$

At a low volume fraction, ϕ , the sedimentation velocity of uncharged particles, U , varies linearly with ϕ according to Batchelor (1972),

$$\frac{U}{U_0} = 1 + k\phi, \quad (3)$$

the constant k , which consists of a relatively large negative contribution from the backflow (-5.5), a small positive effect from the pressure gradient ($+0.5$), and the hindrance due to the near-field hydrodynamics (-1.55), is calculated by Batchelor (1972, 1982) for monodispersed hard spheres to be $k = -6.55$. For non-hard-sphere particles or at higher concentrations, the value of k deviates from -6.55 (Batchelor, 1972; Russel et al., 1989), which results from the interparticle interactions. For attractive interparticle interactions, k is smaller than -6.55 , while for repulsive interparticle interactions, k is larger than -6.55 (Batchelor, 1972; Russel et al., 1989; Thies-Weesie et al., 1995). Recently, Lionberger and Russel (1997) have incorporated the many-body thermodynamic interactions into their model to calculate the hydrodynamic interactions between monodisperse hard spheres.

For bidispersed systems, the sedimentation velocity of uncharged hard spheres of species i through a dispersion of spheres of species j depends on both the volume fractions ϕ_i and ϕ_j . Batchelor (Batchelor, 1982; Batchelor and Wen, 1982) calculated the relevant coefficients S_{ii} and S_{ij} for bidispersed hard spheres at low volume fractions to be

$$\frac{U_i}{U_0} = 1 + S_{ii}\phi_i + S_{ij}\phi_j, \quad (4)$$

where U_0 is the single-particle sedimentation velocity of an i -sphere, as is defined in Eq. 2; S_{ii} is equal to -6.55 , as in Eq. 3; and S_{ij} accounts for the hydrodynamic interactions due to the presence of the j -spheres. The expression of S_{ij} is rather complicated (Batchelor, 1982). However, in the case of a large-size ratio, R_i/R_j , S_{ij} can be approximated by

$$S_{ij} \approx \frac{-5}{2} - \gamma, \quad (5)$$

where the particle density ratio $\gamma = (\rho_j - \rho_0)/(\rho_i - \rho_0)$. The factor $5/2$ in Eq. 5 stems from the presence of small spheres, j , producing an increase in the viscosity according to Einstein's

relation $\eta = \eta_0(1 + 2.5\phi)$. A similar approach, in which a bimodal dispersion with a large-particle-size ratio is treated as a large-particle suspension in a continuous medium consisting of fluid and small particles, was taken by Farris (1968), and Sengun and Probstein (1989) in their research. The factor γ partly originates from a retarding backflow induced by any sedimentation of small spheres j . The additional buoyancy force resulting from the greater density of the medium due to the presence of the j spheres is also included in γ . All effects retard the sedimentation velocity of the large i spherical particles.

Theoretical model for interparticle interactions in colloidal systems

We chose a bidispersed particle suspension whose structure and stability are the target of our study. The small particles may represent solvent molecules, ions, or just small colloidal particles, which can modify the interaction between large particles, the packing structure of large particles, and eventually the stability behavior of the system. We shall ignore the depletion force of the large particles themselves since their concentration is very low (2 vol. %) in our case.

The potential of mean force $U(r)$ between two large hard spherical particles immersed in a fluid made up of small particles can be calculated from the radial distribution function $g(r)$ (Hunter, 1987),

$$U(r) = -kT \ln g(r). \quad (6)$$

To evaluate the effective pair interaction between two large particles, we first need to know the radial distribution function according to Eq. 6. The O-Z theory (Ornstein and Zernike, 1914) provides a theoretical approach to calculate the radial distribution function in a many-body system. It simply states that the total correlation function $h(r)$, which is related to the radial distribution function $g(r)$ by $h(r) = g(r) - 1$, consists of two parts. The first part is the direct correlation between these two particles denoted by $c(r)$, and the second part is contributed by all possible indirect correlations through the other particles in the system. The latter can be expressed exactly as the convolution of the direct correlation function and the total correlation function.

For a binary mixture of large hard spheres and the small hard spherical particles, we assume that the small particles, with polydispersity P , have a Gaussian distribution,

$$n_i \propto \exp\left[-(d_i - d)^2 / 2\sigma^2\right], \quad (7)$$

where σ is the mean square deviation,

$$\sigma = \sqrt{\sum (d_i - d)^2 n_i / \sum n_i}, \quad (8)$$

σ determines the polydispersity P (standard deviation) of the system,

$$P = \sigma/d, \quad (9)$$

and d is the average diameter of small particles,

$$d = \frac{\sum n_i d_i}{\sum n_i}. \quad (10)$$

In the actual calculations, due to the difficulties in dealing with a system with continuous particle distribution (corresponding to a system with an infinite number of different sizes), a finite, discrete distribution was used to fit the continuous Gaussian distribution. Thus, the system was confined to a finite number of different particle sizes.

The bare-pair interaction between two hard-sphere particles in a bidispersed system can be represented as

$$U(r)_{ij} = \begin{cases} \infty, & r < d_{ij} \\ 0, & r > d_{ij} \end{cases}, \quad (11)$$

where $d_{ij} = (d_i + d_j)/2$ is the center-to-center distance between particle i and particle j when they are in contact.

Similar to a monodispersed system, the O-Z integral equation can also be used to express the particle-particle interaction in a mixture,

$$h_{ij}(r_{12}) = c_{ij}(r_{12}) + \sum_{l=1}^P \left(\frac{\rho_l}{\rho} \right) \int \rho_l h_{il}(r_{13}) c_{lj}(r_{32}) dr_3, \quad (12)$$

where ρ_l is the density of particle type l , c_{ij} is the direct correlation between particles i and particle j , and h_{ij} is the total correlation function between particles i and j .

In order to solve the preceding O-Z equation, an appropriate closure relation between the two correlation functions $h_{ij}(r)$ and $c_{ij}(r)$ is needed. A generalized Percus-Yevick (1958) equation for mixtures is used in this model,

$$[h_{ij}(r) + 1][1 - \exp(U_{ij}(r)/kT)] = c_{ij}(r). \quad (13)$$

In this study, we use the Baxter factorization method (Baxter, 1970) to calculate the radial distribution function $g_{ii}(r)$ between large particles. The detailed numerical method to implement Baxter's method in a computer calculation is described elsewhere (Chu et al., 1996).

Results and Discussion

In order to investigate the depletion and structural forces inside a bidispersed colloidal system, sedimentation experiments were performed with a mixture of silica particles. Sets of silica dispersions were prepared in identical tubes, all containing the same amount of large-silica particles ($d = 330$ nm, and $\phi = 2$ vol. %). The concentration of small-silica particles ($d = 38$ nm and polydispersity 15%) varied in each dispersion from 0 vol. % to 40 vol. %. The dispersion of large particles appeared to be white and could easily settle at $20 \pm 0.1^\circ\text{C}$, while the dispersion of small particles was transparent and stable (unsedimentable). Thus, the sedimentation of large particles was easily observable. To make the measurement more accurate, a laser beam was used to determine the sedimentation separation boundary based on the observed transition of the backlight scattering patterns from the random scattering pattern formed above the boundary (without larger particles) to the ring-shaped halo pattern formed below the

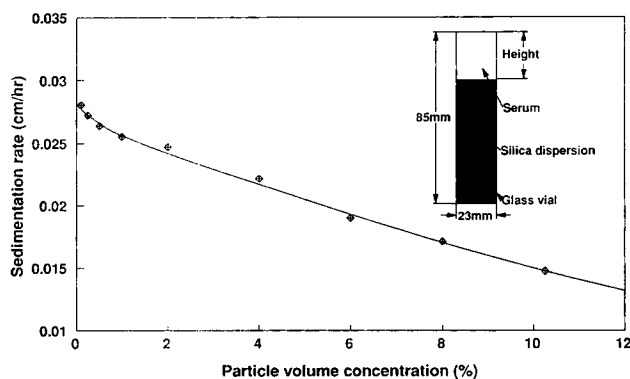


Figure 2. Sedimentation velocity of monodispersed silica particles as a function of the volume concentration.

Silica particle diameter: 330 nm.

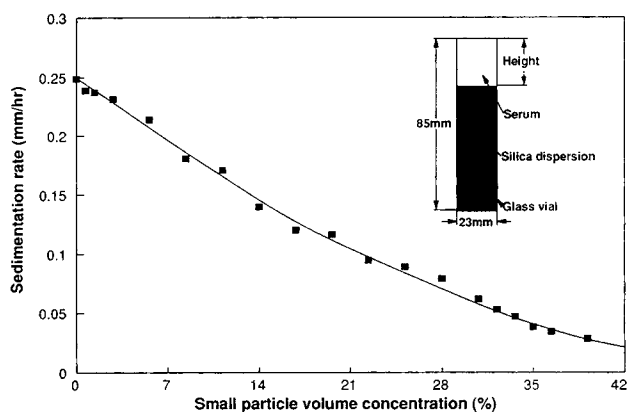


Figure 4. Sedimentation velocity of large particles as a function of the small-particle volume concentration.

Silica size ratio: 330 nm/38 nm and large silica volume fraction: 2%.

boundary (with larger particles). The details of the backlight scattering patterns, theory, and applications can be found elsewhere (Tomita et al., 1982; Xu et al., 1997).

To ensure that the contribution to the depletion force by the large particles themselves in the experiment was negligible due to the very low volume fraction (2 vol. %), sedimentation experiments of monodispersed silica particles (particle diameter 330 nm) were carried out. Figure 2 shows the experimental sedimentation velocity as a function of the particle-volume fraction (0 ~ 12 vol. %). It was found that when the particle-volume fraction increases, the sedimentation rate of particles decreases. This decrease in the rate of sedimentation is mainly the result of the hydrodynamic interaction due to backflow between particles during settling, and has been thoroughly investigated by Batchelor both experimentally (Batchelor, 1972) and theoretically (Batchelor, 1982; Batchelor and Wen, 1982). After we accounted for the effect of backflow using Eq. 3, the normalized sedimentation rate U/U_0 of the silica particles as a function of its volume concentration is shown in Figure 3. The value of U_0 , which is defined as the single-particle sedimentation velocity at infinite dilution, is determined from the extrapolation of sedimentation speed U to infinite dilution, as shown in Figure 2. From this

figure it was observed that, at a low particle-volume concentration (less than 3 vol. %), the normalized sedimentation speed after taking into account the effect of backflow is equal to 1, indicating that at low particle concentrations, Eq. 3 holds. Therefore, the contribution to the depletion force by the large particles themselves in bidispersed dispersions can be ignored, and only the interactions between large particles and small particles are important.

The sedimentation speed as a function of small-particle volume concentration is illustrated in Figure 4. The sedimentation rate decreases with an increase in fine-silica-particle volume fraction due to the viscosity increase of the fine-silica dispersions.

To assess the effect of the viscosity of the small-silica-particle dispersions on the sedimentation rate of large particles, the viscosity of the small-silica-particle dispersions was measured. Due to the non-Newtonian behavior of silica dispersions at high concentrations, the measurement was carried out with caution, ensuring that the dispersions were subjected to the same shear rate (very low) under the measurement conditions as under the sedimentation experiment.

In this research, the viscosity of small-silica-particle dispersions at a very low shear rate was estimated from Stokes' law. Figure 5 illustrates the method of measurement: in this experiment, the small-particle concentration was kept constant, and the large-silica-particle concentration was varied. The viscosity η_0 was obtained from the infinite dilute sedimentation rate U_0 by extrapolating the sedimentation rate curve to zero volume fraction,

$$\eta_0 = \frac{2R^2(\rho_p - \rho_0)g}{9U_0}, \quad (14)$$

where R is the large-silica-particle diameter, ρ_p the large-particle density, ρ_0 the density of small-silica-particle dispersions, and g the gravitational acceleration.

To check the reliability of the preceding method, a Cannon-Fenske-type viscometer (size 100, Cannon Instrument Co.) was also employed to estimate the viscosity of small-

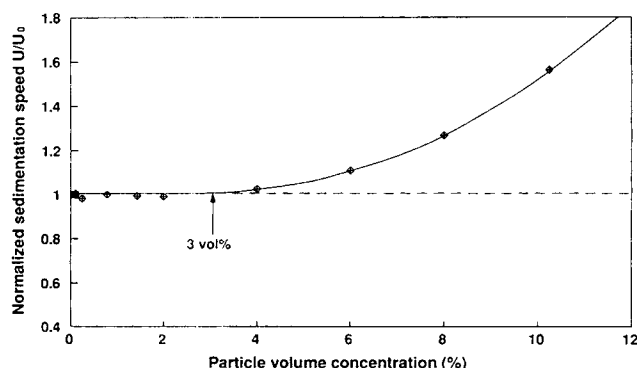


Figure 3. Normalized sedimentation speed U/U_0 corrected for the effect of backflow as a function of the particle volume concentration.

Silica particle diameter: 330 nm.

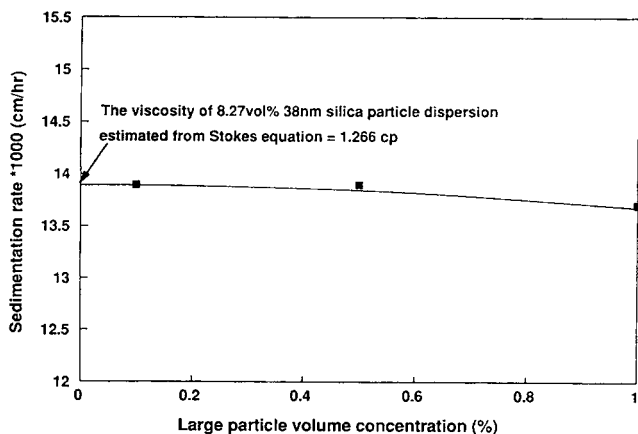


Figure 5. Viscosity estimation of small-silica-particle dispersions from the sedimentation speed of large particles.

Size ratio: 330 nm/38 nm.

silica-particle dispersions. In this method, the time was measured for 6.2 mL of dispersion to flow through a capillary under gravity. The product of this time and the density of the sample is proportional to the viscosity. Due to the strong temperature dependence of the viscosity, the capillary is placed in a thermostat maintained at a temperature of $20 \pm 0.1^\circ\text{C}$. The results obtained from both methods are shown in Figure 6. A very small difference was observed between these two methods, demonstrating that the viscosity data are reliable.

To reveal the effect of the depletion and structural forces on the large-particle sedimentation speed, the sedimentation speeds were first adjusted for the effect of backflow between large particles according to Eq. 3, then the effect of the viscosity and density of small-particle dispersion on the normalized sedimentation rate were also rectified according to the Stokes equation. Figure 7 shows the corrected normalized sedimentation rate U/U_0 as a function of small-particle volume fraction; here U_0 is the single-particle sedimentation velocity at infinite dilution for pure water.

Batchelor's theory for a bidispersed system was compared

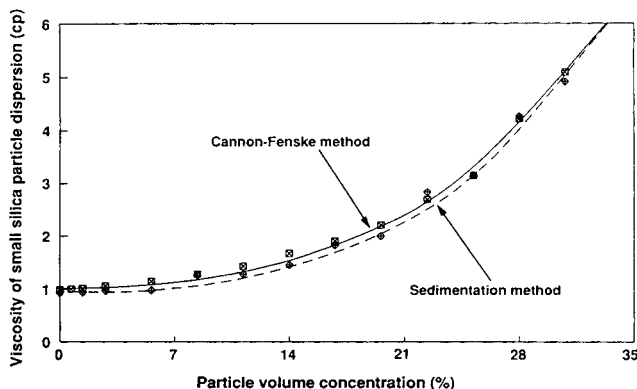


Figure 6. Viscosity of small-particle dispersion as a function of the small-particle volume concentration.

Silica-particle diameter: 38 nm.

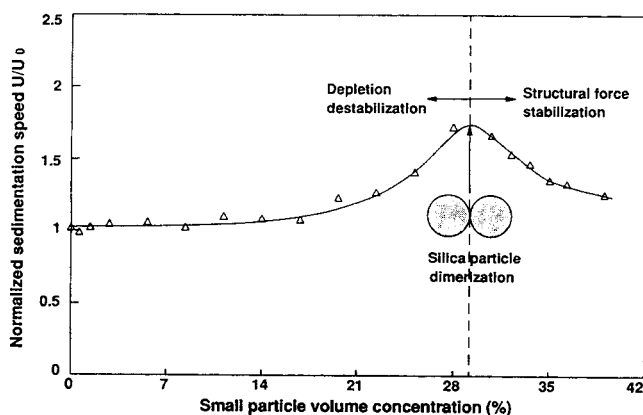


Figure 7. Normalized sedimentation speed U/U_0 corrected for the effect of backflow, density, and viscosity as a function of the small-particle volume concentration.

Silica size ratio: 330 nm/38 nm and large-particle volume concentration: 2%.

with the experimental data. It was found that at a low concentration of small particles (less than 2 vol. %), Eq. 4 holds for a bidispersed system. At a higher small-particle concentration, a large deviation occurs due to the existence of strong interparticle interactions between small and large particles inside the dispersion.

Figure 7 shows very clearly that by increasing the small-particle volume fraction while keeping the large-particle concentration constant, the normalized sedimentation rate U/U_0 increases and finally reaches a maximum around 30 vol. % of fine-particle concentration. After that, the normalized sedimentation rate decreases. The same phenomenon was also observed for the effective diameter of aggregates, as illustrated in Figure 8. In this figure, the effective diameter of aggregates was calculated from the Stokes equation by assuming that the aggregates have the same density as a single particle,

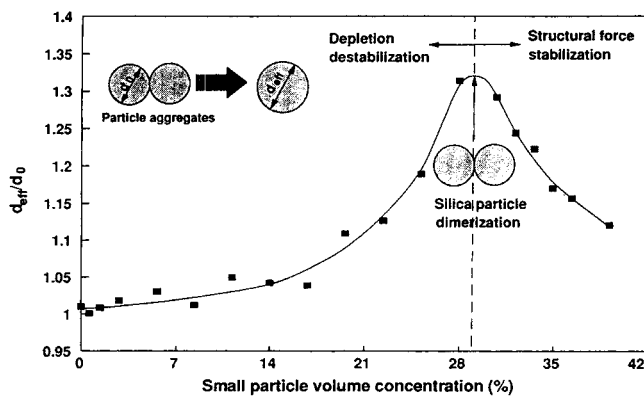


Figure 8. Effective diameter of aggregates as a function of the small-particle volume concentration assuming that the aggregates have the same density as a single particle.

Silica size ratio: 330 nm/38 nm and large-particle volume concentration: 2%.

$$\frac{d_{\text{eff}}}{d_0} = \sqrt{\frac{U}{U_0}} \quad (15)$$

To explain this destabilizing-stabilizing behavior caused by fine particles, we used the theoretical model discussed earlier for a bidispersed hard-sphere system (in which small particles were polydispersed). All the parameters used in these simulations were the same as those in the sedimentation experiment. Figure 9 shows the depletion well depth and structural energy barrier between large particles as a function of the small-particle volume concentration. It is observed that both the depletion well depth and the structural energy barrier increase with the fine-particle volume concentration, but the initial values of the structural energy barrier are very small compared to the thermal energy. In this case, the energy barrier can be easily overcome, and the effect of depletion exceeds the effect of the structural energy barrier; as a consequence, the attractive depletion force pushes the two large particles together and the degree of particle aggregation increases with the increase in fine-particle volume concentration. With a further increase of the fine-particle concentration, the structural energy barrier increases. Finally, the structural energy barrier reaches near 2 kT at 30 vol. % of the fine particles due to the formation of microlayering of small particles around large particles. In this case, before the large particles can get close enough to go into the depletion well, they have to pass through this energy barrier, that is, they have to break the small-particle layer formed between them. Therefore, the degree of the large-particle aggregation decreases. Finally the structural energy barrier (much greater than 5 kT) becomes strong enough to completely inhibit the large-particle aggregation by further increase of small-particle concentration (higher than 45 vol. %), and the dispersion becomes stable.

It is worth pointing out that Woutersen and de Kruif (1993) found a similar phenomenon in their study of the viscosity of semidilute, bidisperse suspensions of hard spheres. The viscosity of bidisperse suspensions (particle-size ratios around

3 ~ 4) was plotted against the composition, and a maximum was observed. The origin of the viscosity maximum can be attributed to the depletion and structural forces.

To estimate the number of particles in an aggregate in our experimental system, some calculations were performed. According to Hiemenz (1986), the friction factor of a prolate ellipsoid in a stationary state sedimentation can be expressed as

$$\frac{f}{f^*} = \frac{\left[1 - \left(\frac{b}{a}\right)^2\right]^{1/2}}{\left(\frac{b}{a}\right)^{2/3} \ln \left[\frac{1 + \left[1 - \left(\frac{b}{a}\right)^2\right]^{1/2}}{\frac{b}{a}} \right]} \quad (16)$$

where f^* is the friction factor of a sphere that has the same volume as the prolate ellipsoids, and b/a is the ratio of the equatorial semiaxis to the semiaxis of a revolution sphere.

A dimer can be approximated as a prolate ellipsoid with $b/a = 0.5$. Then the friction factor of a doublet can be estimated from the preceding equation, and the normalized sedimentation speed U/U_0 in an infinite dilute system is calculated from the Stokes equation to be

$$\frac{U}{U_0} = 1.52, \quad (17)$$

where U_0 is the sedimentation rate of a single particle in an infinite dilute dispersion.

This value of 1.52 is very close to the experimental normalized sedimentation speed U/U_0 at the maximum point in Figure 7, which indicates that most of the aggregates in our experimental system were dimers.

Summary

The depletion and structural forces in a bidispersed, low-charged colloidal dispersion have been experimentally investigated. The depletion destabilization and structural barrier stabilization mechanisms were observed. Theoretical calculations were carried out to explain the experimental results using the O-Z method. A good qualitative agreement between the experiment and the theory was obtained.

Notation

- d_i = particle diameter of i sphere, m
- p = constant
- r = distance, m
- s = variable
- S_{ii}, S_{ij} = constant
- z = variable

Literature Cited

- Aronson, M. P., "The Role of Free Surfactant in Destabilizing Oil-in-Water Emulsions," *Langmuir*, **5**, 494 (1989).
- Aronson, M. P., "Flocculation of Emulsions by Free Surfactant in Purified Systems," *Colloids Surf.*, **58**, 195 (1991).

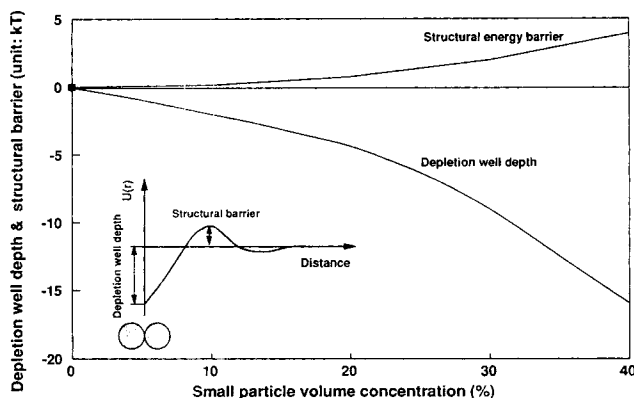


Figure 9. Depletion-well depth and structural energy barrier between two large particles as a function of small-particle volume concentration calculated from the Ornstein-Zernike method for hard spheres.

Silica size ratio: 330 nm/38 nm, large silica volume concentration: 2% and small-particle polydispersity: 15%.

- Aronson, M. P., "Surfactant Induced Flocculation of Emulsions," *Emulsions—A Fundamental and Practical Approach*, J. Sjöholm, ed., Ser. C, Math. and Phys. Sci., Vol. 363, p. 75 (1992).
- Asakura, S., and F. Oosawa, "On Interaction Between Two Bodies Immersed in a Solution of Macromolecules," *J. Chem. Phys.*, **22**, 1255 (1954).
- Asakura, S., and F. Oosawa, "Interaction Between Particles Suspended in Solutions of Macromolecules," *J. Polym. Sci.*, **33**, 183 (1958).
- Basheva, E. S., A. D. Nikolov, P. A. Kralchevsky, I. B. Ivanov, and D. T. Wasan, "Multi-stepwise Drainage and Viscosity of Macroscopic Films Formed from Latex Suspensions," *Surfactants Solutions*, **II**, 467 (1992).
- Batchelor, G. K., "Sedimentation in a Dilute Dispersion of Spheres," *J. Fluid Mech.*, **52**, 145 (1972).
- Batchelor, G. K., "Sedimentation in a Dilute Polydisperse System of Interacting Spheres, Part 1. General Theory," *J. Fluid Mech.*, **119**, 379 (1982).
- Batchelor, G. K., and C. S. Wen, "Sedimentation in a Dilute Polydisperse System of Interacting Spheres: 2. Numerical Results," *J. Fluid Mech.*, **124**, 495 (1982).
- Baxter, R. J., "Ornstein-Zernike Relation and Percus-Yevick Approximation for Fluid Mixtures," *Phys. Rev.*, **52**, 4559 (1970).
- Bergeron, V., and C. J. Radke, "Equilibrium Measurements of Oscillatory Disjoining Pressures for Thin Liquid Foam Films," *Langmuir*, **8**, 3023 (1992).
- Bibette, J., D. Roux, and F. Nallet, "Depletion Interactions and Fluid-Solid Equilibrium in Emulsions," *Phys. Rev. Lett.*, **65**, 2470 (1990).
- Bibette, J., "Depletion Interactions and Fractionated Crystallization for Polydisperse Emulsion Purification," *J. Colloid Interf. Sci.*, **147**, 474 (1991).
- Chu, X. L., A. Nikolov, and D. T. Wasan, "Monte Carlo Simulation of In-Layer Structure Formation in Thin Liquid Films," *Langmuir*, **10**, 4403 (1994).
- Chu, X. L., A. D. Nikolov, and D. T. Wasan, "Thin Liquid Film Structure and Stability: The Role of Depletion and Surface-Induced Structural Forces," *J. Chem. Phys.*, **103**, 6653 (1995).
- Chu, X. L., A. D. Nikolov, and D. T. Wasan, "Effects of Particle Size and Polydispersity on the Depletion and Structural Forces in Colloidal Dispersions," *Langmuir*, **12**, 5004 (1996).
- Dickinson, E., M. J. Goller, and D. J. Wedlock, "Osmotic Pressure, Creaming, and Rheology of Emulsions Containing Nonionic Polysaccharide," *J. Colloid Interf. Sci.*, **172**, 192 (1995).
- Dickinson, E., M. Golding, and M. J. W. Povey, "Creaming and Flocculation of Oil-in-Water Emulsions Containing Sodium Caseinate," *J. Colloid Interf. Sci.*, **185**, 515 (1997).
- Dominique, M., D. M. E. Thies-Weesie, A. P. Philipse, and H. N. W. Lekkerkerker, "Sedimentation of Bidisperse, Uncharged Colloidal Sphere Suspensions: Influence of Viscosity and Irregular Surfaces," *J. Colloid Interf. Sci.*, **177**, 427 (1995).
- Farris, R. J., "Prediction of the Viscosity of Multimodal Suspensions from Unimodal Viscosity Data," *Trans. Soc. Rheol.*, **12**, 281 (1968).
- Feigin, R. I., and D. H. Napper, "Depletion Stabilization and Depletion Flocculation," *J. Colloid Interf. Sci.*, **75**, 525 (1980).
- Gast, A. P., C. K. Hall, and W. B. Russel, "Phase Separations Induced in Aqueous Colloidal Suspensions by Dissolved Polymer," *Faraday Discuss. Chem. Soc.*, **76**, 189 (1983).
- Hiemenz, P. C., *Principles of Colloidal and Surface Chemistry*, 2nd ed., Dekker, New York and Basel (1986).
- Hunter, R. J., *Foundations of Colloidal Science*, Vols. I, II, Oxford Univ. Press, New York (1989).
- Koczko, K., A. D. Nikolov, D. T. Wasan, R. P. Borwankar, and A. Gonsalves, "Layering of Sodium Caseinate Sub-micelles in Thin Liquid Films: A New Stability Mechanism for Food Dispersions," *J. Colloid Interf. Sci.*, **178**, 694 (1996).
- Liang, W., Th. F. Tadros, and P. F. Luckham, "Investigations of Depletion Flocculation of Concentrated Sterically Stabilized Latex Dispersions Using Viscoelastic Measurements and Microscopy," *J. Colloid Interf. Sci.*, **158**, 152 (1993).
- Lionberger, R. A., and W. B. Russel, "A Smoluchowski Theory with Simple Approximations for Hydrodynamic Interactions in Concentrated Dispersions," *J. Rheol.*, **41**, 399 (1997).
- Mao, Y., M. F. Cates, and H. Lekkerkerker, "Depletion Force in Colloidal Systems," *Physica A*, **222**, 10 (1995).
- Nikolov, A. D., and D. T. Wasan, "Ordered Micelle Structuring in Thin Film Formed from Anionic Surfactant Solutions: I. Experimental," *J. Colloid Interf. Sci.*, **133**, 1 (1989).
- Nikolov, A. D., P. A. Kralchevsky, I. B. Ivanov, and D. T. Wasan, "Ordered Micelle Structuring in Thin Film Formed from Anionic Surfactant Solutions: II. Model Development," *J. Colloid Interf. Sci.*, **133**, 13 (1989).
- Nikolov, A. D., and D. T. Wasan, "Dispersion Stability Due to Structural Contributions to the Particle Interaction as Probed by Thin Liquid Film Dynamics," *Langmuir*, **8**, 2985 (1992).
- Nikolov, A. D., and D. T. Wasan, "Particle-Particle Interactions in Concentrated Dispersions as Probed by the Capillary Force Balance with Application to Batch Sedimentation," *Powder Tech.*, **88**, 299 (1996).
- Nikolov, A. D., and D. T. Wasan, "Effects of Film Size and Micellar Polydispersity on Film Stratification," *Colloids Surf.*, in press (1997).
- Ornstein, L. S., and F. Zernike, *Proc. Acad. Sci. (Amsterdam)*, **17**, 793 (1914).
- Percus, J. K., and G. J. Yevick, "Analysis of Classical Statistical Mechanics by Means of Collective Coordinates," *Phys. Rev.*, **110**, 1 (1958).
- Richetti, P., and P. Kekicheff, "Direct Measurement of Depletion and Structural Forces in Micellar System," *Phys. Rev. Lett.*, **68**, 1951 (1992).
- Russel, W. B., D. A. Saville, and W. R. Schowalter, *Colloidal Dispersions*, Cambridge Univ. Press, New York (1989).
- Sanyal, S., N. Easwar, S. Ramaswamy, and A. K. Sood, "Phase Separation in Binary Near-Hard-Sphere Colloids: Evidence for the Depletion Force," *Europhys. Lett.*, **18**, 107 (1992).
- Seebergh, J. E., and J. C. Berg, "Depletion Flocculation of Aqueous, Electrosterically Stabilized Latex Dispersions," *Langmuir*, **10**, 454 (1994).
- Sengun, M. Z., and R. F. Probstein, "Bimodal Model of Slurry Viscosity with Application to Coal-Slurries: 1. Theory and Experiment," *Rheol. Acta*, **28**, 382 (1989).
- Tadros, Th. F., "Concentrated Sterically Stabilized Dispersions and Their Flocculation by Depletion Layers," *Prog. Colloid Poly. Sci.*, **83**, 36 (1990).
- Tomita, M., K. Takano, and T. G. M. van de Van, "An Optical Method for Studying the Properties of Ordered Lattices," *J. Colloid Interf. Sci.*, **92**, 367 (1983).
- Walz, J. Y., and A. Sharma, "Effect of Long Range Interactions on the Depletion Force between Colloidal Particles," *J. Colloid Interf. Sci.*, **168**, 485 (1994).
- Woutersen, A. T. J. M., and C. G. de Kruif, "The Viscosity of Semidilute, Bidisperse Suspensions of Hard Spheres," *J. Rheol.*, **37**, 681 (1993).
- Xu, W., A. D. Nikolov, D. T. Wasan, A. Gonsalves, and R. P. Borwankar, "Particle Structure and Stability of Colloidal Dispersions as Probed by the Kossel Diffraction Technique," *J. Colloid Interf. Sci.*, **191**, 4710 (1997).

Manuscript received Apr. 9, 1997, and revision received July 24, 1997.